

Development of normalized liquefaction resistance curve for clean sands

Saeed-ullah Jan Mandokhail¹ · Duhee Park¹ · Jin-Kwon Yoo¹

Received: 10 February 2016 / Accepted: 26 September 2016 / Published online: 4 October 2016
© Springer Science+Business Media Dordrecht 2016

Abstract We present empirically derived liquefaction resistance curve from a large database of measurements from published literature and also simple shear tests that were performed in this study. The data measured from simple shear and triaxial tests are separately compiled. The data are fitted with two empirical models to develop representative liquefaction resistance curves. Comparisons illustrate that the slope of the widely used power law is highly dependent on the range of data it is fitted to and that the power law underestimates the resistance at high number of cycles (N). The alternative empirical model is demonstrated to provide favorable fit with the measurement over a wide range of data. The representative curves are normalized by the equivalent number of uniform cycles for a magnitude (M) 7.5 event ($N_{M=7.5}$) to reduce the wide scatter of the measurements and to make it usable with liquefaction triggering charts that relate in situ parameter with cyclic resistance ratio for a $M = 7.5$ event. Comparison with published liquefaction resistance curves show that the proposed curve is lower at $N \leq N_{M=7.5}$ and higher at $N > N_{M=7.5}$. A single-parameter empirical exponential function that closely fits the normalized liquefaction resistance curves and representative values for its parameter are presented. We also propose an empirical equation to correct the liquefaction resistance curve measured from a triaxial test to match that from a simple shear test.

Keywords Liquefaction resistance curve · Cyclic resistance ratio · Number of cycles · Cyclic simple shear test · Cyclic triaxial test

1 Introduction

Stress-controlled cyclic tests are routinely performed to produce an empirical relationship between applied uniform cyclic stress and number of cycles required to trigger liquefaction (N). The amplitude of the cyclic stress is typically normalized by the effective overburden

✉ Duhee Park
dpark@hanyang.ac.kr

¹ Department of Civil and Environmental Engineering, Hanyang University, Rm 506 Jaesung Civil Engineering Building, Haengdang-dong, Sungdong-gu, Seoul 133-791, Republic of Korea

stress (effective vertical stress for a simple shear test and effective mean stress for a triaxial test) to produce a cyclic stress ratio (CSR). CSR that triggers liquefaction in a specified number of cycles is termed the cyclic strength or the cyclic resistance ratio (CRR). The relationship between CRR and N is termed the cyclic strength curve (Ishihara 1996; Kramer 1996) or the liquefaction resistance curve (Towhata 2008).

The liquefaction resistance curve is used as the weighting factor curve to calculate the equivalent number of uniform cycles (N_{eq}) from an irregular time series, as proposed by Seed et al. (1975). N_{eq} is also the underlying basis of the magnitude scaling factor and used with liquefaction triggering correlations that relate in situ soil parameter with CRR to assess the liquefaction potential (e.g. Boulanger and Idriss 2004, 2012; Idriss and Boulanger 2008, 2010; Seed et al. 1984, 1985). Seed et al. (1975) used the CRR versus N data of De Alba et al. (1976) as the weighting factor curve. Liu et al. (2001) used the compiled CRR versus N data measured from simple shear tests to calculate N_{eq} . The data were fitted with an empirical two-parameter power law. Idriss and Boulanger (2006) used the data of Yoshimi et al. (1984, 1989) to determine N_{eq} . The cyclic triaxial test results of Yoshimi et al. (1984, 1989) on frozen soil samples were also fitted with the power law. Kishida and Tsai (2014) used the curve of Idriss and Boulanger (2006) to calculate N_{eq} . Boulanger and Idriss (2015b) evaluated the influence of the liquefaction resistance curve on the magnitude scaling factor. Recently, the liquefaction resistance curve is being used to calibrate numerical pore pressure models. Boulanger and Ziotopoulou (2015) proposed to use the liquefaction curve to evaluate and select the input parameters of their plasticity soil model. For stress-based pore pressure models (e.g. Ivšić 2006; Park et al. 2014), the liquefaction curve is the key input parameter.

As summarized, the liquefaction curve is an essential input to assess the liquefaction potential. However, there is a large uncertainty in the shape of the curve and therefore, a wide range of curves have been used. The effects of soil parameters and test methods need to be better quantified. We also need to look in more detail the applicability of the power law that has most frequently been used to fit the CRR versus N data, because it was reported that the slope of the model is highly dependent on the range of data over which it is fitted (Boulanger and Idriss 2015b).

We conducted a series of laboratory tests and performed a comprehensive literature review to collect and quantify reported liquefaction resistance curves for various types of clean sands. The effects of the type of test, relative density, confining pressure, and sample preparation method on the shape of the liquefaction curve are investigated. The measured data points are fitted to the power law and another empirical model, and their relative accuracies are compared. From the data, representative liquefaction resistance curves are presented. The proposed curves are compared to previously reported range of curves. A predictive equation for the liquefaction resistance curve that best fits the measurement is proposed. Finally, we propose an empirical equation to correct the liquefaction curve measured from a triaxial test to match that from a simple shear test.

2 Liquefaction resistance curve

The liquefaction resistance curve is obtained from stress-controlled cyclic triaxial (TX) or simple shear tests (SS). The liquefaction triggering in a stress-controlled test is defined as the state at which the residual excess pore water pressure ratio (r_u) exceeds a target value (Cetin and Bilge (2012) or when the maximum shear or axial strain exceeds a threshold

value (Ishihara 1993; Jiaer et al. 2004). It was reported that the cyclic resistance measured from cyclic triaxial tests and simple shear tests are not equivalent (Castro 1975; Finn et al. 1971; Seed et al. 1975; Seed and Peacock 1971). Triaxial tests resulted in higher cyclic resistances to liquefaction and flatter curves compared with cyclic simple shear tests, as shown in Fig. 1.

Because the stress field imposed in a simple shear test is recognized to be the most representative of the field stress path under a vertically propagating shear wave, CRR from a triaxial test, $(CRR)_{TX}$, is corrected to match that from a simple shear test, $(CRR)_{SS}$, as follows:

$$(CRR)_{SS} = c_r(CRR)_{TX} \tag{1}$$

where c_r is the correction factor. Various forms of c_r have been proposed, as summarized in Table 1. It should be noted that the correction factor only shifts the curve vertically, and does not change the slope of the curve.

The following empirical equation is widely used to define the relationship between CRR and N :

$$CRR = aN^{-b} \tag{2}$$

where a and b are curve fitting parameters. The empirical curve has been widely used to fit the measured CRR and N data points. Liu et al. (2001) used the cyclic simple shear test measurements from a large body of literature, which include the data of Tatsuoka and Silver (1981), De Alba et al. (1976), Ishihara and Yamazaki (1980), and Boulanger and Seed (1995). In Fig. 2, the data of Tatsuoka and Silver (1981) are fitted to the power law. As discussed in the previous section, it is shown that the slope is highly dependent on the range of N the curve is fitted to. If the data at $N > 20$ is included, b becomes considerably lower. Comparisons demonstrate that a linear log (CRR) versus log (N) correlation does not successfully fit the data for a wide range of N and that a unique value for the parameter b cannot be obtained. Figure 3 displays all simple shear test data used in the study of Liu et al. (2001). CRR of the data are normalized to CRR at $N = 15$, denoted $CRR_{N=15}$. Also shown in the figure is the upper and lower bounds of the data, as proposed by Liu et al. (2001). The upper bound curve, which has a b value of 0.37, was used as the laboratory-based weighting factor curve to determine N_{eq} . Comparisons show that the measured data fall below the upper bound curve at $N < 15$ and are higher than the curve at $N > 15$. The

Fig. 1 Comparison of cyclic strength of Monterey sand measured from triaxial test and simple shear test (Peacock and Seed 1968)

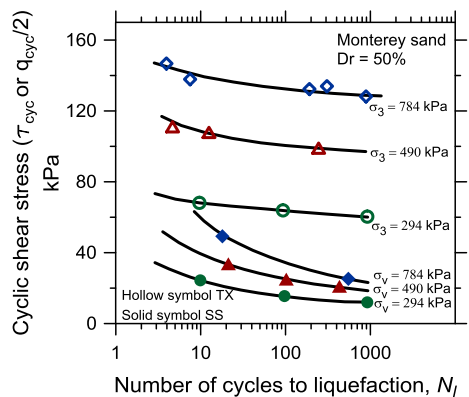


Table 1 Correction factors used to adjust liquefaction resistance curve from cyclic triaxial tests

Correction factor	References
$c_r = \frac{(1+2K_\sigma)}{3}$	Seed and Peacock (1971)
$c_r = \frac{(1+K_\sigma)}{2}$	Finn et al. (1971)
$c_r = \frac{2(1+2K_\sigma)}{3\sqrt{3}}$	Castro (1975)

Fig. 2 Best fit curves using the power law to the data points from Tatsuoka and Silver (1981)

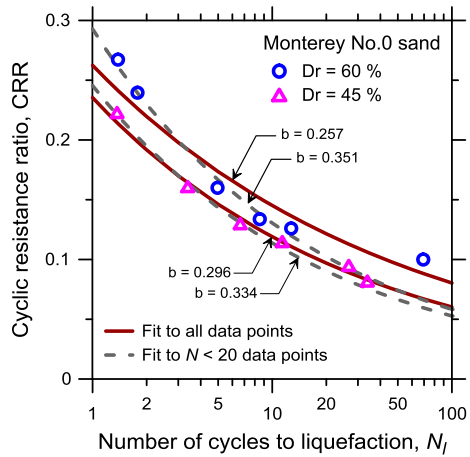
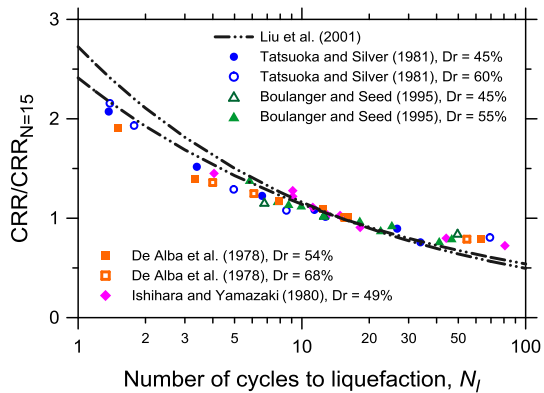


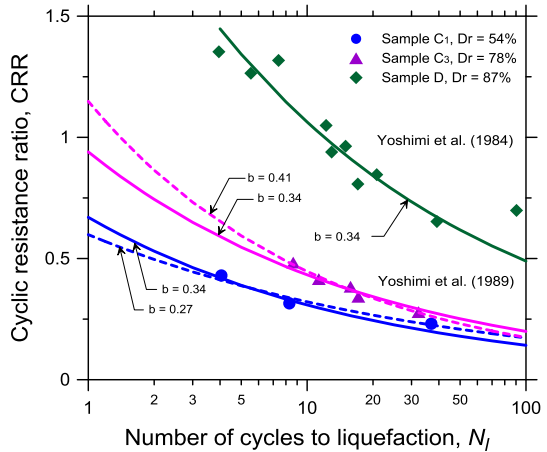
Fig. 3 Comparison of the SS band of Liu et al. (2001) and the normalized CRR data (CRR normalized to $CRR_{N=15}$) used by Liu et al. (2001)



match is particularly not agreeable at high values of N . This is because the power law fitted to the data at low N greatly underestimates the resistance at high N .

Idriss (1999) used the data of Yoshimi et al. (1984), whereas Idriss and Boulanger (2006) used the data of Yoshimi et al. (1984, 1989) shown in Fig. 4 to determine the b parameter of the power law. In the study of Idriss and Boulanger (2006), the data set was grouped into dense ($D_r = 87\%$) and medium dense sands ($D_r = 54, 78\%$). It was reported in both Idriss (1999) and Idriss and Boulanger (2006) that the b values for all densities were 0.34. Using the same data set, Boulanger and Idriss (2015b) reported that the value of b ranges from 0.13 to 0.41. The main difference between two studies is the range of N used to fit the data, again highlighting the limitation of the power law. Boulanger and

Fig. 4 TX tests on frozen sample from Yoshimi et al. (1984, 1989) fitted with *b* values reported by Idriss and Boulanger (2006) and Boulanger and Idriss (2015b)



Idriss (2015b) addressed that the data from two other sets of cyclic triaxial tests on clean sands produced *b* values ranging from 0.10 and 0.25. The values of the *b* parameter that fit three sets of cyclic simple shear test results ranged from 0.08 to 0.27. The values of the *b* parameter fitted to the simple shear test results was shown to be lower than those fitted to the data of Yoshimi et al. (1984, 1989). Possible reasons for the wide variation in the *b* values for the simple shear test results were not discussed. For some sets of measurements, the data are clustered within a narrow range of *N*, which may have biased the value of *b*. It may have been influenced by the limited number of CRR versus *N* data to which the power law curve was fitted to. It was also reported that for curves that become strongly curved at low number of cycles, the power law approximation may not be adequate. The representative values of *b* for which the magnitude scaling factors were derived were 0.40, 0.34, 0.28, 0.22, and 0.16. The values represent a broad range of soil types including clean, silty, and clayey sands. Kishida and Tsai (2014) used *b* = 0.34 as the reference slope of sands in calculating *N*_{eq}.

The most widely used values of the *b* parameter for clean sands, as reported in previous studies, are 0.34 and 0.37. However, it should also be noted that the values are close to the upper bound of the measured data at low *N*. It should also be highlighted that they provide poor fits at high number of cycles, because a linear relationship between log (CRR) and log (*N*) is assumed. As discussed in the previous section, because the formulation does not imply an asymptotic trend for CRR at high *N*, the residual pore pressure is predicted to develop even at very small levels of shear stress. This contradicts the findings from physical experiments that illustrate that at stress amplitudes below a threshold value, the residual pore water pressure does not develop and liquefaction will not be triggered, irrespective of the number of stress cycles (Dobry et al. 1982; Vucetic 1994).

Empirical liquefaction resistance curve can also be constructed using the damage parameter (*D*) of Park et al. (2014), which is defined as follows:

$$D = (\eta/CSR)(CSR - CSR_t)^\alpha \tag{3}$$

where *CSR*_{*t*} = threshold shear stress ratio below which residual pore pressure is not generated, η = length of shear stress path [equivalent to 4 *N*·(*CSR*) for cyclic stress-controlled tests], α = calibration parameter. Two parameters, *CSR*_{*t*} and α , are selected such that *D* is a constant for a given liquefaction curve. The selection procedure of two

parameters, as outlined in Park et al. (2014), is as follows. Initially, a value of CSR_t is assumed. The exponent α is determined from the following equation:

$$\alpha_{avg} = \frac{\sum_{i=1}^{M-1} \left\{ \frac{\log\left(\frac{N_i}{N_{i+1}}\right)}{\log(CSR_{i+1}-CSR_t) - \log(CSR_i-CSR_t)} \right\}}{M} \tag{4}$$

where M is number of data points of the CRR versus N curve, i and $i + 1$ denote two adjacent data points of the curve. The equation is derived from Eq. (3) and represents the mean of the parameter α across the CRR versus N data. This process is repeated over a range of CSR_t until α that results in the lowest COV is obtained. After the parameters CSR_t and α are selected, the corresponding D_{avg} is again calculated. The damage parameter equation can be reformulated to produce a relationship between CRR and N .

$$CSR = \left(\frac{D_{avg}}{4N}\right)^{1/\alpha_{avg}} + CSR_t \tag{5}$$

The equation provides an alternative method to express the liquefaction resistance curve. However, representative values for CSR_t , α , and D_{avg} were not proposed.

3 Compilation of measured liquefaction resistance curves

In this section, the measured CRR versus N curves digitized from published literature are compiled and compared. The list of referred literature, soil properties, and details of the tests are summarized in Table 2. We also performed cyclic simple shear tests on reconstituted specimens of clean Ottawa and Jumunjin sands. Ottawa sand is a standard quartz sand designated as ASTM C 778 (ASTM 1995) (also known as ASTM C 109). Jumunjin sand is a standard sand used in Korea. The maximum and minimum void ratios e_{max} and e_{min} were determined according to ASTM D4254 (ASTM 2006b) and ASTM D4253 (ASTM 2006a), respectively. The physical properties of both sands are listed in Table 2. The specimens were 6.37 cm in diameter and 2.4 cm in height, which satisfies the ASTM D6528-07 (ASTM 2007) requirements. Moist tamping method was used to prepare the reconstituted samples. We used NGI-type wire reinforced membrane. All samples were anisotropically consolidated under 100 kPa. After consolidation, the samples were sheared under uniform 0.1 Hz sinusoidal stress. The tests were performed at three relative densities for both Ottawa and Jumunjin sands.

The relative densities of all measured test data range from 15 to 87 %, and the confining pressures range from 50 to 400 kPa. Sample preparation methods used include water pluviation, air pluviation, moist tamping by under compaction, slurry deposition, and saturated tamping. It should be noted that only tests results on clean sands were used in this study. As reported in Cetin and Bilge (2012), the cyclic resistance is dependent on the strain threshold or r_u used to define liquefaction triggering. The values used in their study ranges from single amplitude (SA) shear strain = 1 to 6 % and r_u from 0.5 to 0.9. The liquefaction triggering criteria used in the compiled data set are summarized in Table 2. It is shown that for simple shear tests, the range of shear strain threshold is narrow, which are double amplitude (DA) = 5, 6, and 7.5 %, and SA = 3 and 3.75 %. For triaxial tests, all data that we compiled used DA axial strain = 5 %. Only 2 test data among a total of 28

Table 2 Summary of soil properties of CRR–N curves used in this study

Soil	Type of test ^a	Dr (%)	Confining pressure ^b (kPa)	G _s	D ₅₀ (mm)	C _u	e _{max}	e _{min}	Sample preparation method	Liquefaction triggering criteria	References
Jumunjin sand	SS	40, 61, 80	100	2.65	0.53	1.49	0.985	0.638	Moist tamping	5 % DA	This study
Ottawa sand	SS	40, 60, 80	100	2.65	0.31	1.89	0.764	0.49			This study
Monterey No. 0 sand	Large scale SS	54, 68, 82	55	2.65	0.36	1.5	0.85	0.56	Dry pluvial	i _u = 1.0	De Alba et al. (1976)
Fraser river sand	SS	40, 59, 72	50, 100, 200, 400	2.72	0.30	NR	1.00	0.68	Water pluviation	3.75 % SA	Sivathayalan (1994)
Fraser river sand	SS	40	100	2.72	0.26	1.6	0.94	0.62	Air pluviation	3.75 % SA	Sriskandakumar (2004)
Nevada sand	SS	64	NR	NR	NR	NR	0.94	0.55	Low density: Air pluviation	3.75 % SA	Brandes and Seidman (2008)
Maui dune sand	SS	37, 51	NR	NR	NR	NR	0.83	0.61	High density: Tamping		
Kawahae Harbor sand	SS	24, 67	NR	NR	NR	NR	1.05	0.64			
Algeria sand	SS	15, 55, 75	100	2.69	0.31	1.76	0.89	0.53	Moist tamping with 5 % water	3.75 % SA	Da Fonseca et al. (2015)
Coimbra sand	SS	15, 45, 65	100	2.66	0.36	2.13	0.81	0.48			
Modified Sacramento river sand	Bidirectional SS	35, 45, 55	207	2.68	NR	1.3	1.01	0.64	Moist tamping	3 % SA	Boulanger and Seed (1995)
Fuji river sand	SS	49	200	2.728	0.40	3.16	1.03	0.48	Water pluviation	3 % SA	Ishihara and Yamazaki (1980)

Table 2 continued

Soil	Type of test ^a	Dr (%)	Confining pressure ^b (kPa)	G _s	D ₅₀ (mm)	C _u	e _{max}	e _{min}	Sample preparation method	Liquefaction triggering criteria	References
Monterey No. 0 sand	SS	45, 60	100	2.65	0.36	1.5	0.85	0.56	Moist tamping	7.5 % DA	Tatsuoka and Silver (1981)
Monterey 0/30 sand	SS	35, 45, 60, 80	40, 80, 180	2.64	0.36	1.29	0.89	0.541	Water pluviation	6 % DA	Jiaer et al. (2004)
Hokksund sand	TX	30, 57	125	2.71	NR	2.04	0.95	0.61	Moist tamping	5 % DA	Tadesse (2000)
Ottawa sand	TX	40, 67, 77, 82	100	2.65	0.31	1.89	0.78	0.48	Slurry deposition	5 % DA	Carraro et al. (2003)
Silica No.8 sand	TX	65, 73, 79	100	2.645	0.084	2.46	1.381	0.721	Saturated tamping	5 % DA	Zhou et al. (2009)
Sacramento river sand	TX	38, 59.5, 76	98	2.68	NR	1.27	1.03	0.61	NR	r _u = 1.0	Lee and Seed (1967)
Babolsar sand	TX	12, 37.6, 59	200	2.78	0.24	1.8	0.83	0.55	Moist tamping	5 % DA	Ahmadi and Paydar (2014)
Firoozkooh sand	TX	46.5, 66.6, 83	200	2.65	0.23	1.32	0.89	0.64			
Niigata sand	TX	57, 83	98	2.69	0.29	1.8	1.2	0.77	Air pluviation	5 % DA	Tokimatsu et al. (1986)
Monterey sand	TX	43, 58, 65, 81	100	2.65	0.43	1.5	0.821	0.631	Moist tamping	5 % DA	Polito (1999)
Yatesville sand	TX	11, 26, 68	100	2.72	0.18	2.4	0.972	0.653			
Toyoura sand	TX	20, 50	100, 300	2.64	0.216	1.392	0.977	0.605	Moist tamping	5 % DA	Yang and Sze (2011)
Monterey No.0 sand	TX	60	100	2.65	0.36	1.5	0.85	0.56	Moist tamping	5 % DA	Silver et al. (1976)

Table 2 continued

Soil	Type of test ^a	Dr (%)	Confining pressure ^b (kPa)	Gs	D ₅₀ (mm)	C _u	e _{max}	e _{min}	Sample preparation method	Liquefaction triggering criteria	References
Natural Niigata sand	TX	54	78	2.74	0.23	1.6	1.06	0.671	Frozen sample	5 % DA	Yoshimi et al. (1989)
Natural Niigata sand	TX	78	98	2.77	0.25	1.4	1.05	0.668	Frozen sample	5 % DA	
Niigata sand	TX	87	98	2.68	0.28	1.9	1.197	0.752	Frozen sample	5 % DA	Yoshimi et al. (1984)

NR not reported

^a SS, cyclic simple shear test; TX, cyclic triaxial test

^b Effective mean stress in triaxial test and effective vertical stress in simple shear test

data sets applied the r_u criterion. Because of the relative uniformity in the strain threshold and the limited sets of data that used the r_u criterion, we believe that the effect of the liquefaction triggering criteria is not significant and its effect on the shape of the liquefaction curve does not need to be accounted for.

Figures 5 and 6 display the liquefaction resistance curves measured from simple shear tests (9 out of 14 sands) and triaxial tests (9 out of 14 sands), respectively. Due to limitation in space, not all results of tests as summarized in Table 2 are displayed. Based on the measured data points, the liquefaction resistance curves were constructed using the model of Park et al. (2014) and the power law to fit the data points.

For simple shear tests, Fig. 5 confirms that sand type, density, confining pressure, and sample preparation techniques influence the cyclic resistance, as reported by (Ladd 1974; Mulilis et al. 1977; Peacock and Seed 1968; Silver and Park 1976). The cyclic resistance is

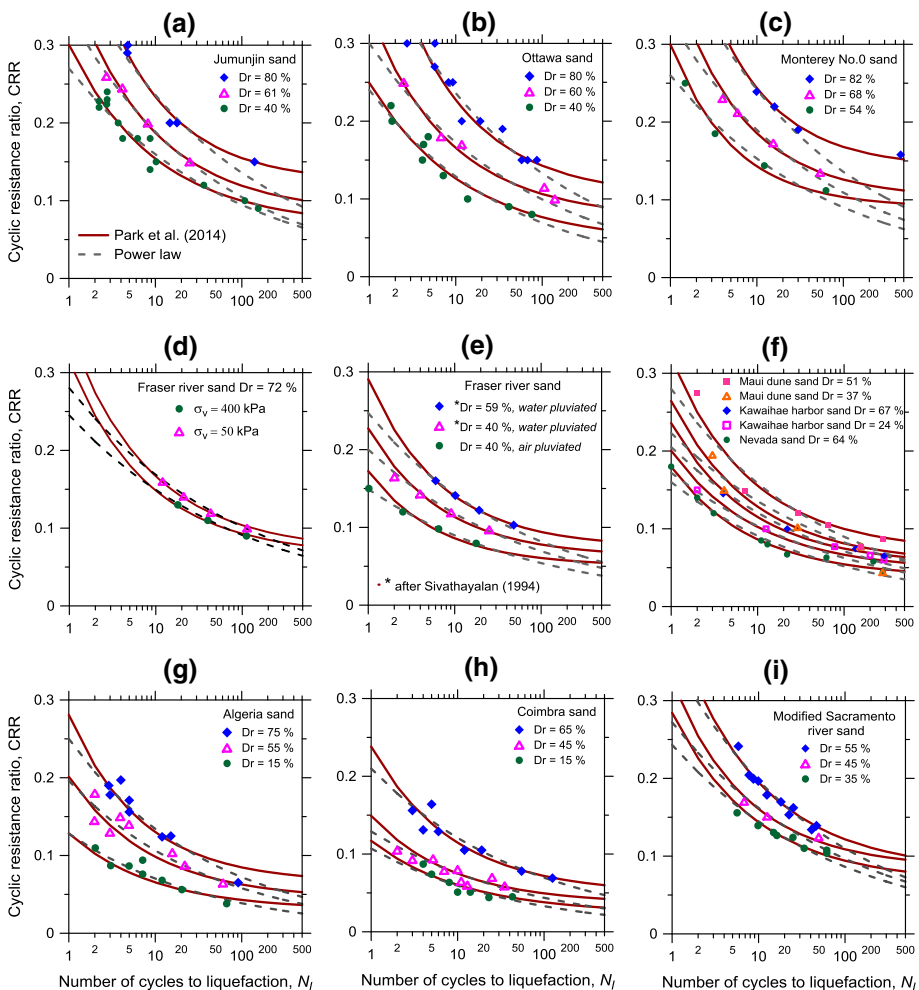


Fig. 5 Relationship between CRR and N for clean sands measured from stress-controlled cyclic simple shear tests. *Solid lines* and *dashed lines* represent fitted CRR versus N curves constructed by the Park et al. (2014) model and power law, respectively

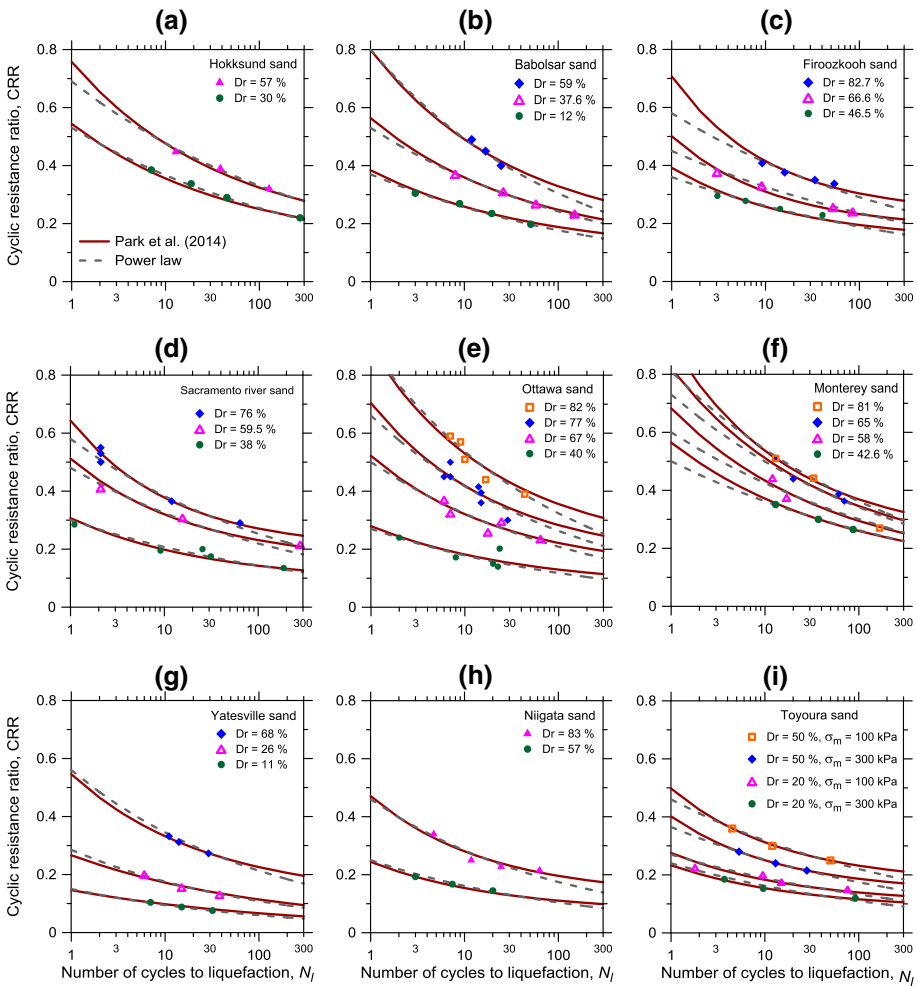


Fig. 6 Relationship between CRR and N for clean sands measured from stress-controlled cyclic triaxial tests. *Solid* and *dashed* lines represent fitted CRR versus N curves constructed by the Park et al. (2014) model and power law, respectively

shown to increase with an increase in the relative density or a decrease in the void ratio. A decrease in CRR with increase in the confining pressure is observed, as shown in Fig. 5d. The decrease is more significant for dense sands. Water pluviated samples show higher resistance to liquefaction than the sample prepared by air pluviation, as illustrated in Fig. 5e. The liquefaction resistance curves constructed by the model of Park et al. (2014) and power law are shown in Fig. 5. The model of Park et al. (2014) is shown to produce better matches with the measurements. The power law is shown to underestimate CRR at high N values, because the power law assumes a linear relationship between CRR and N in log–log plot and CRR reduces to zero at high values of N . As discussed in the previous section, it contradicts the observation that the residual pore pressure does not develop at strains below the threshold volumetric strain and corresponding CSR_t (Dobry et al. 1982; Vucetic 1994). Park et al. (2014) model is shown to capture this behavior realistically.

Overall, Park et al. (2014) model produces a higher and steeper curve at $N \leq 2$ and $N > 20$ than when using the power law.

The measured CRRs from triaxial tests, Fig. 6, are shown to be generally larger than those from simple shear tests, and at the same time the curves are flatter. This is in line with the discussion given in the previous section that the liquefaction curve from a triaxial test is higher than that from a simple shear test (Fig. 1), and that $(CRR)_{TX}$ needs to be corrected. As observed in the results of simple shear tests, pronounced influences of the relative density and confining pressure are also observed.

4 Normalized liquefaction resistance curves

In this section, we present the liquefaction resistance curve that are normalized to CRR at $N_{M=7.5}$, which represents N_{eq} for a $M = 7.5$ event. The rationale behind this normalization is to develop curves that are usable with the semi-empirical liquefaction triggering curves which correlate in situ parameter with $CRR_{M=7.5}$, where $CRR_{M=7.5}$ represents the resistance ratio for a $M = 7.5$ event (e.g. Andrus et al. 2009; Andrus and Stokoe II 2000; Boulanger and Idriss 2014, 2015a; Cetin et al. 2004; Idriss and Boulanger 2012; Kayen et al. 2013; Moss et al. 2006; Seed et al. 1985). To normalize, we need to estimate the representative value of $N_{M=7.5}$.

Seed et al. (1975) and Idriss (1999) addressed that $N_{M=7.5} = 15$, based on the data of De Alba et al. (1976) and Yoshimi et al. (1984, 1989), respectively. Liu et al. (2001) reported that $N_{M=7.5}$ is critically dependent on the distance from fault rupture (R_{rup}) and the CRR versus N relationship, and that the site class and near-fault rupture directivity have secondary influences. Representative $N_{M=7.5}$ was 23 for $R_{rup} < 30$ km. Green and Terri (2005) performed nonlinear site-response analyses and calculated N_{eq} based on the dissipated energy. N_{eq} was shown to be functions of M , R_{rup} , and depth in a soil profile. Idriss and Boulanger (2008) addressed that for simplicity the value of N_{eq} may be expressed solely as a function of earthquake magnitude and recommended to use $N_{M=7.5} = 15$. Boulanger and Idriss (2015b) analyzed the effect of b on N_{eq} and showed that the geometric mean of $N_{M=7.5}$ is relatively constant at 15 for b values between 0.2 and 0.5. Kishida and Tsai (2014) analyzed more than 3500 ground motion records for site class D conditions and investigated the influence of the peak ground acceleration (PGA), a spectral ratio parameter describing the shape of the acceleration responses spectra, M , R_{rup} , parameter b , and the period of the soil layer. The proposed empirical function is the following:

$$\ln N_{eq} = \ln \left[\frac{\exp(c_0 + c_1 \ln PGA + c_2 \ln S_1 + c_3 M + c_4 \ln b + c_5 b T_s) + 0.5}{0.65^{1/b}} \right] \quad (6)$$

where $c_0 = -3.43$; $c_1 = -0.352$; $c_2 = -0.402$; $c_3 = 0.798$; $c_4 = 1.72$; and $c_5 = -1$; S_1 is the spectral ratio between S_a at 1.0 and 0.2 s, $PGA =$ peak ground acceleration in unit of g , and $T_s = 4z/\bar{V}_s$ ($\bar{V}_s =$ average shear wave velocity from the ground surface to the depth z). Their analysis also showed that N_{eq} increases with R_{rup} . The geometric mean of $N_{M=7.5}$ for $R_{rup} < 40$ km [most of the liquefaction case histories documented by Seed et al. (2001) are within this range], is approximately 15 for $PGA = 0.2$ g , as shown in Fig. 7a. $N_{M=7.5}$ is shown to decrease with increase in PGA and T_s . It is shown that b has a secondary influence on $N_{M=7.5}$ relative to R_{rup} . Based on previous studies, we recommend to use $N_{M=7.5} = 15$ if estimates of R_{rup} , PGA , and T_s are not available. If representative

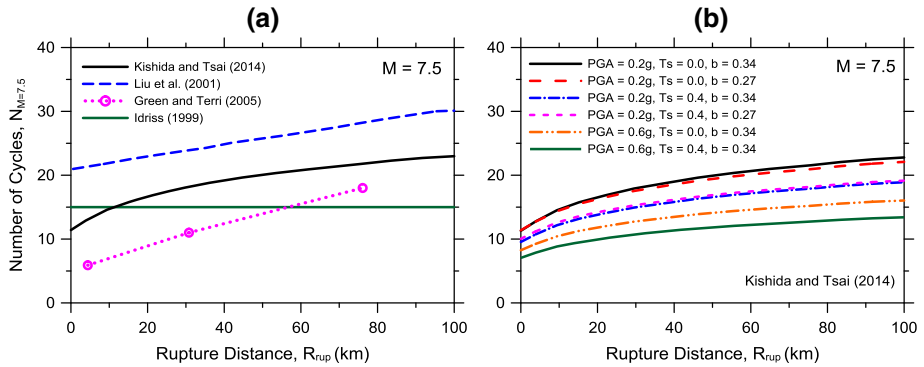


Fig. 7 Comparison of $N_{M=7.5}$ **a** comparison of $N_{M=7.5}$ proposed by Idriss (1999), Liu et al. (2001), Green and Terri (2005), and Kishida and Tsai (2014) [PGA = 0.2 g, $b = 0.34$, and $T_s = 0.0$], **b** effect of PGA, T_s and b on calculated $N_{M=7.5}$ using the equation of Kishida and Tsai (2014)

values for all parameters are available, the empirical equation of Kishida and Tsai (2014) can be used to determine $N_{M=7.5}$.

In the ensuing, we firstly present the liquefaction resistance curves normalized to $CRR_{N=15}$. Curves normalized to values of $N_{M=7.5}$ other than 15 will be presented in the following section. The normalized liquefaction resistance curves from simple shear tests are shown in Fig. 8. Only curves fitted by the model of Park et al. (2014) are shown, because it fits more favorably with the measured data. The scatter of CRR is significantly decreased when normalized. The curves are dependent on the relative density, where the normalized curve increases with increase in the relative density. The curves, however, are independent of the confining pressure and sample preparation method, as shown in Fig. 8d and e, respectively. Normalized curves from triaxial tests data fitted with Park et al. (2014) model are also shown in Fig. 9. The normalized curves from triaxial tests are all lower compared with those from simple shear tests, because the measured curves are flatter.

Figure 10a, b display all normalized curves measured by simple shear and triaxial tests, respectively. The mean curves for both sets of data were calculated and are shown in Fig. 10. The variability about the mean curve was quantified by the standard deviation (σ), as shown in Fig. 11. The standard deviations for both simple shear and triaxial test measurements are demonstrated to be quite small, where the maximum value of the standard deviation is only 0.8. Due to the small value of the standard deviation, we produce the two standard deviation curves to represent the uncertainty in the normalized curve, as illustrated in Fig. 10a, b. In Fig. 10a, the power law curves with $b = 0.34$ and 0.37 are also illustrated for comparison purposes. As has been described in the previous section, the $b = 0.34$ curve was used by Idriss (1999) and Idriss and Boulanger (2006), whereas the $b = 0.37$ curve was used by Liu et al. (2001). The power law curves are shown to be higher than the proposed mean curve at $N < 15$ and lower at $N > 15$. The proposed plus two standard deviation curve is shown to be close to the Idriss (1999) curve, but slightly lower at $N < 15$ and steeper from $N = 1$ to 3. The mean curve is best approximated by $b = 0.28$, although it will underestimate CRR at $N = 1$ and $N > 15$. The plus and minus two standard deviation curves are most favorably approximated by $b = 0.31$ and 0.25 , respectively.

The normalized curves from triaxial tests, Fig. 10b, are greatly lower and flatter than those from simple shear tests, as described previously and shown in Fig. 9. The parameter b that best fits the mean curve is 0.19. The plus and minus two standard deviation curves

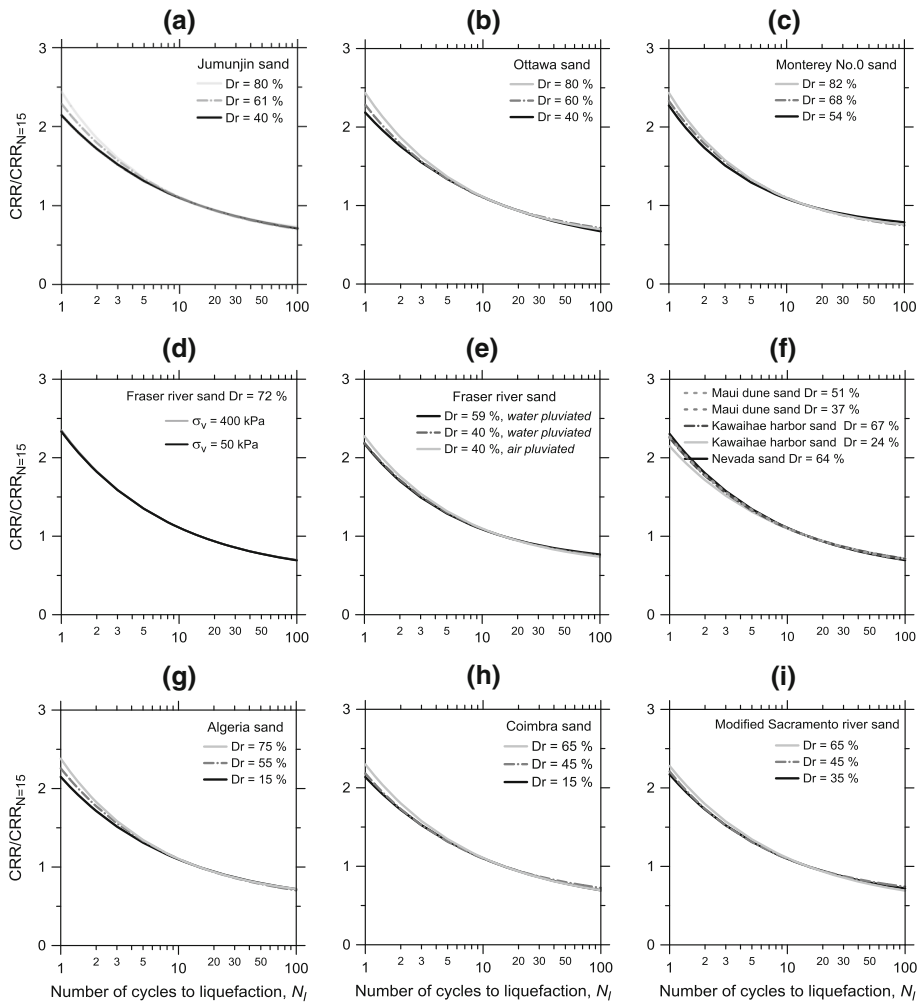


Fig. 8 $CRR/CRR_{N=15}-N$ curves fitted with Park et al. (2014) model to data from simple shear tests

are fitted most agreeably by $b = 0.22$ and 0.15 , respectively. In calculating the mean and two standard deviation curves, the data of Yoshimi et al. (1984, 1989) were not included. The $b = 0.34$ curve, which fits the normalized data of Yoshimi et al. (1984, 1989) is shown to be significantly higher and steeper than all other triaxial test measurements. The curves match more favorably with the simple shear test results, as discussed in the previous section. We considered the results of Yoshimi et al. (1984, 1989) as outliers, and therefore they were not included in deriving the representative curves for the triaxial tests.

Because $N_{M=7.5}$ is not a fixed value and varies as a function of various parameters including the rupture distance, we need to develop liquefaction resistance curves that are normalized by values other than 15. In Fig. 12, the measurements are normalized by $N_{M=7.5} = 20$ and 23 , respectively. As for the case of $N_{M=7.5} = 15$, the measurements are shown to collapse into narrow bands. However, the slope of the curve varies depending on the value of $N_{M=7.5}$.

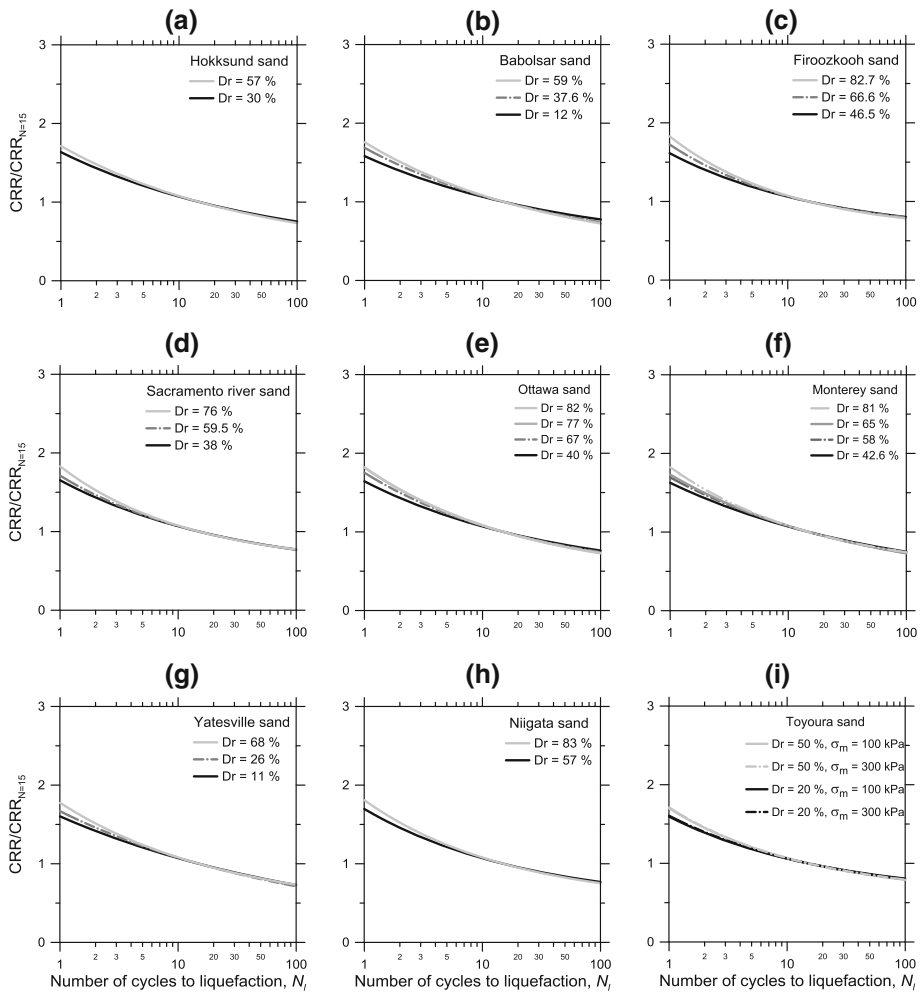


Fig. 9 $CRR/CRR_{N=1.5}$ – N curves fitted with Park et al. (2014) model to data from triaxial tests

Development of the normalized curves with the Park et al. (2014) model, although more accurate than the power law, can be difficult in practice because it requires multiple parameters. To make the normalized data more accessible, a new empirical function for the liquefaction resistance curve that closely matches the measurements is proposed as follows:

$$\frac{CRR}{CRR_{M=7.5}} = \frac{e^{(N_{M=7.5}/N)^c}}{e^{(1)}} \tag{7}$$

where c is a curve fitting parameter. It should be noted that different values of c should be assigned for $N \leq N_{M=7.5}$ and $N > N_{M=7.5}$ slopes. The equation can be used for any value of estimated $N_{M=7.5}$, but the corresponding c values will also vary accordingly. The values of c for mean, and two standard deviations for $N_{M=7.5}$ value ranging from 10 to 30 are

Fig. 10 Comparison of $CRR/CRR_{N=15}-N$ curves: **a** simple shear tests data fitted with Park et al. (2014) model, **b** triaxial test data fitted with Park et al. (2014) model. The $b = 0.34$ and $b = 0.37$ power law curves are also shown for comparison purposes

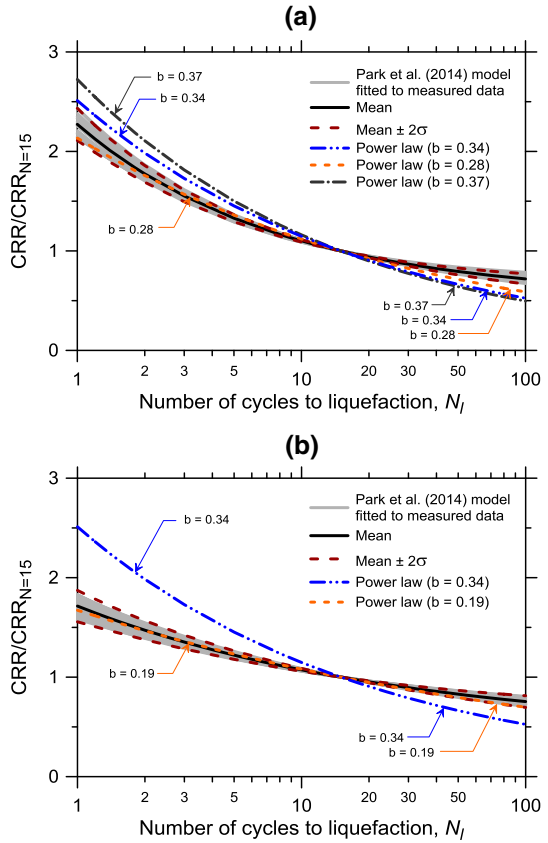
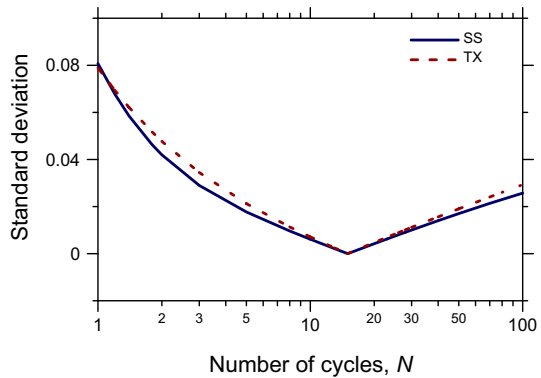


Fig. 11 Standard deviation of $CRR/CRR_{N=15}-N$ curves



displayed in Fig. 13. The values of c for representative $N_{M=7.5}$ are also summarized in Table 3.

As shown in Figs. 8 and 9, the normalized curves from simple shear tests are steeper and lie above the normalized curves from triaxial tests at $N < 15$. Because the liquefaction resistance curve from the simple shear test can be considered to be more representative, triaxial test results are most often corrected to match those from simple shear tests. The

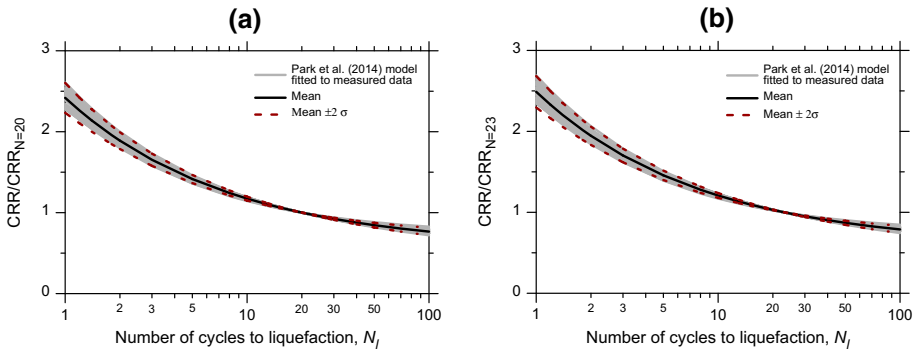


Fig. 12 Simple shear tests data fitted with Park et al. (2014) model **a** $CRR/CRR_{N=20}$ - N curves, **b** $CRR/CRR_{N=23}$ - N curves

Fig. 13 Variation of parameter c of Eq. (7) for mean and two standard deviation liquefaction curves with $N_{M=7.5}$

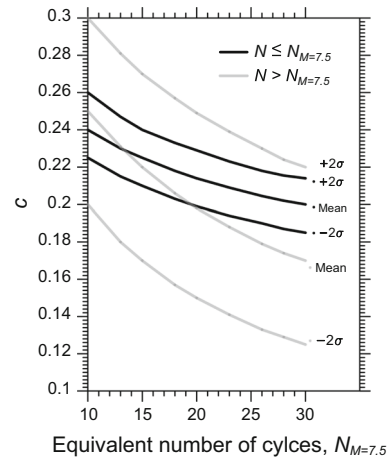


Table 3 Proposed values for the parameter c of Eq. (7)

	$N \leq N_{M=7.5}$					$N > N_{M=7.5}$				
$N_{M=7.5}$	10	15	20	25	30	10	15	20	25	30
Mean	0.24	0.23	0.21	0.21	0.20	0.25	0.22	0.20	0.18	0.17
Mean + 2σ	0.26	0.24	0.23	0.22	0.22	0.30	0.27	0.25	0.23	0.22
Mean - 2σ	0.23	0.21	0.20	0.19	0.19	0.20	0.17	0.15	0.14	0.13

correction factor summarized in Table 1 accounting for the difference in K_0 , apply a uniform correction value across a wide range of N . However, at higher stress ratios (low number of cycles), it was reported that the cyclic triaxial test results are heavily influenced by the extension part of the stress cycle since the applied stresses tend to lift the cap from the test specimen. This may cause necking near the top of the sample and cause the specimen to fail at lower number of cycles (Seed et al. 1975). To account for this underestimation of the cyclic resistance at low number of cycles, the correction factor

should be higher at lower cycles and gradually decrease with N . A new N dependent function to fit the liquefaction resistance curve from a triaxial test to that from a simple shear test is proposed as follows:

$$c_r^* = (c_r) \times \left(\frac{N_{M=7.5}}{N} \right)^d \tag{8}$$

where c_r is the correction factor summarized in Table 1, and d is a curve fitting parameter. The correction factor increases with a decrease in N , and therefore the corrected curve becomes steeper at low N . The function was developed through regression analysis such that the corrected normalized mean curve from triaxial test fits the normalized mean curve from simple shear test. The best fit value of d for the mean curve and $N_{M=7.5} = 15$ was calculated as 0.07.

To evaluate the accuracy of the proposed correction curve, the curves from simple shear tests and corrected curves based on triaxial test measurements are compared. The liquefaction resistance curves from both simple shear and triaxial tests were available for only Ottawa sand, as summarized in Table 2. It should be noted that different specimen preparation methods were used for respective tests. The moist tamping and the slurry deposition method were used to prepare specimens for simple shear (this study) and triaxial tests (Carraro et al. 2003), respectively. Additionally, the relative densities of the soil samples differ. For the relative densities of specimens were 40, 60, 80 % were for simple shear tests, whereas the soils were tested at densities of 40, 67, and 77 % for triaxial tests.

Figure 14a–c compare the liquefaction resistance curves from simple shear tests and curves corrected with the functions listed in Table 1. The curves corrected by the function

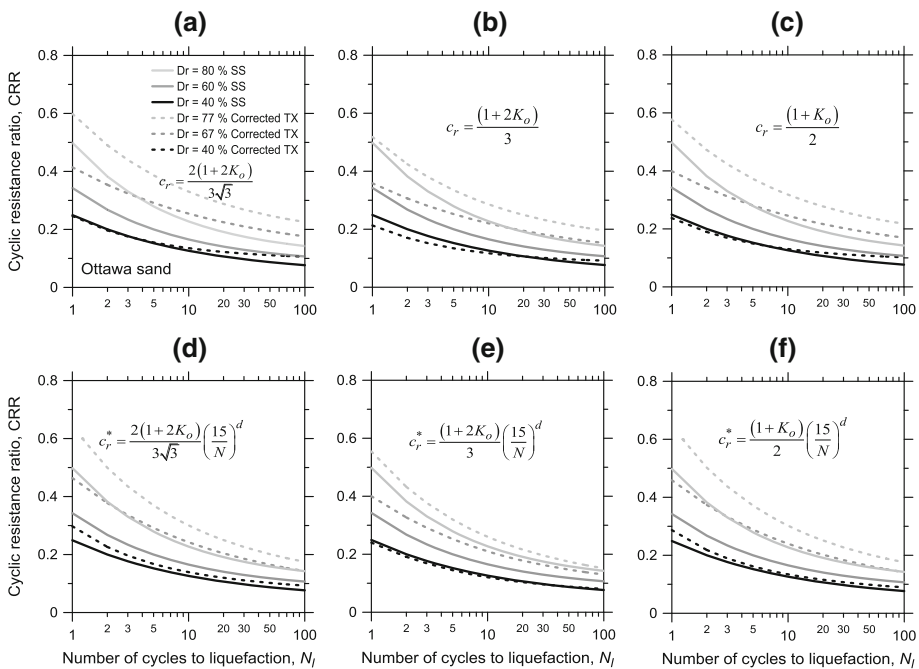
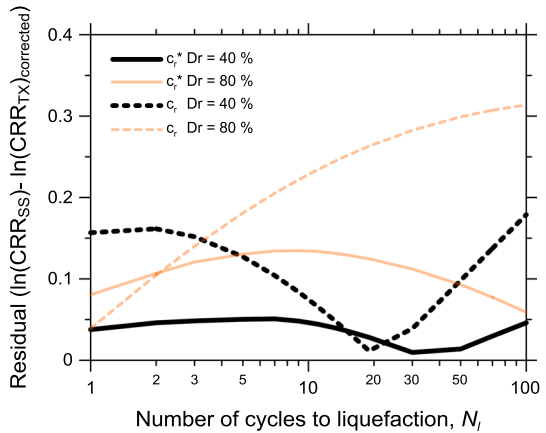


Fig. 14 Comparison of liquefaction resistance curves of Ottawa sand from cyclic simple shear tests and curves from triaxial tests corrected to fit those from SS tests

Fig. 15 Residuals of the corrected liquefaction curves constructed from the triaxial test and the target curve measured from simple shear test, both on Ottawa sand. c_r^* and c_r represents the proposed correction factor and the factor of Seed and Peacock (1971), respectively



of Seed and Peacock (1971) are shown to result in the most favorable matches with the results from simple shear tests, as illustrated in Fig. 14b. However, all the curves from triaxial tests are flatter compared to those from simple shear tests. Figure 14d–f plots the curves corrected with Eq. (8). It is demonstrated that the proposed correction curve produces improved fits with the measurements from simple shear test. The slope of the fitted curves matches very well with the target curves. Again, Fig. 14e results in the best fit with the liquefaction resistance curves obtained from simple shear tests. To quantify the accuracy of two correction factors, the absolute residuals between the target and corrected curves (Fig. 14b, e) are calculated and displayed in Fig. 15. The residuals are calculated for relative densities of 40 and 80 %. When the correction factor of Seed and Peacock (1971) is used, the maximum residuals are up to 0.18 and 0.31 for $Dr = 40$ and 80 %, respectively. However, when the proposed N dependent function is used, the residuals are significantly reduced for both $Dr = 40$ and 80 % specimens to less than 0.05 and 0.14 respectively. Considering differences in the sample preparation method, discrepancy with the target curve is inevitable. However, it is encouraging that the proposed N dependent correction function derived from the mean curves greatly enhances the fit with the simple shear test results for a specific soil.

5 Conclusions

Empirically derived liquefaction resistance curves are presented based on a large database of test results from published literature and simple shear tests that we performed. The measurements from simple shear and triaxial tests are separately compiled to develop respective liquefaction resistance curves. The representative curves that we derived are normalized to reduce the wide scatter of the measurements and to make it usable with liquefaction triggering chart that relate in situ parameter with cyclic resistance ratio (CRR) for a magnitude (M) = 7.5 event. The proposed curves are compared to design curves that have been used to determine the equivalent number of uniform cycles (N_{eq}) and to derive the magnitude scaling factors. The main findings of this study are the following.

1. Two models were used to fit the measured data. The power law, which is most often used, is shown to be flatter than the measurements at low number of cycles and

underestimates the resistance at high number of cycles. The slope of the power law is also demonstrated to be not unique for a set of data, but highly sensitive on the range of data it is fitted to. Additionally, the asymptotic trend of the measurements cannot be realistically captured by the power law. The Park et al. (2014) model is shown to produce very favorable fit with the target measurements. Contrary to the power law, unique sets of parameters for the Park et al. (2014) model that fit a wide range of data can be found.

2. The scatter of CRR is significantly reduced when normalized to CRR at $N_{M=7.5}$ (N_{eq} for a $M = 7.5$ event), denoted $CRR_{M=7.5}$. The wide range of measured liquefaction resistance curves collapses into a narrow band. The normalized curves are dependent on the relative density, where they increase with an increase in the relative density. The normalized curves, however, are independent of the confining pressure and the sample preparation method. The standard deviation of the normalized curves is shown to be lower than 0.08. Therefore, the variability of the normalized curve can be well represented by the proposed mean and two standard deviation curves.
3. The normalized curves from simple shear tests are demonstrated to be lower than the widely used power law based curves at $N < N_{M=7.5}$ and higher at $N > N_{M=7.5}$. The proposed curves are also steeper than the power law based curves at low N . The normalized curves based on triaxial test measurements are shown to be greatly lower and flatter than the simple shear test based curves.
4. We propose an empirical exponential function that closely fit the representative curves produced from the measurements. To account for the pronounced difference in the slope of the normalized liquefaction resistance curve with respect to $N_{M=7.5}$, different values are assigned to the parameter for $N \leq N_{M=7.5}$ and $N > N_{M=7.5}$. Representative values for the parameter of the empirical function for $N_{M=7.5}$ ranging from 10 to 30 are presented in the form of a chart and also a table.
5. Correction factor used in practice to adjust the cyclic liquefaction curve from a triaxial test to account for the K_o condition is shown to be inappropriate because it only shifts the curve vertically and does not modify the slope of the curve. A new correction function that additionally adjusts the slope of the curve as a function of N is proposed. The correction function is validated through measurements from parallel triaxial and simple shear tests using comparable soil specimens.
6. The proposed liquefaction resistance curves can be used to calculate N_{eq} , to develop new sets of magnitude scaling factors, and to calibrate numerical pore pressure models. The shape of the curve may have a secondary influence on N_{eq} , as reported in previous studies, but it is expected to have a primary effect on the magnitude scaling factors. Although it is out of scope of this study, it is an important topic that warrants further investigation.

Acknowledgments This research was supported by Basic Science Research Program through the National Research Foundation of Korea (NRF) funded by the Ministry of Science, ICT and Future Planning (NRF-2015R1A2A2A01006129).

References

- Ahmadi MM, Paydar NA (2014) Requirements for soil-specific correlation between shear wave velocity and liquefaction resistance of sands. *Soil Dyn Earthq Eng* 57:152–163. doi:10.1016/j.soildyn.2013.11.001

- Andrus RD, Stokoe KH II (2000) Liquefaction resistance of soils from shear-wave velocity. *J Geotech Geoenviron Eng ASCE* 126(11):1015–1025. doi:[10.1061/\(ASCE\)1090-0241\(2000\)126:11\(1015\)](https://doi.org/10.1061/(ASCE)1090-0241(2000)126:11(1015))
- Andrus RD, Hayati H, Mohanan NP (2009) Correcting liquefaction resistance for aged sands using measured to estimated velocity ratio. *J Geotech Geoenviron Eng ASCE* 135(6):735–744. doi:[10.1061/\(ASCE\)GT.1943-5606.0000025](https://doi.org/10.1061/(ASCE)GT.1943-5606.0000025)
- ASTM (1995) Standard specification for standard sand. ASTM C 778, West Conshohocken, PA
- ASTM (2006a) Standard test method for maximum index density and unit weight of soils using a vibratory table. ASTM D 4253, West Conshohocken, PA
- ASTM (2006b) Standard test methods for minimum index density and unit weight of soils and calculation of relative density. ASTM D 4254, West Conshohocken, PA
- ASTM (2007) Standard test method for consolidated undrained direct simple shear testing of cohesive soils. D 6528-07, West Conshohocken, PA
- Boulanger RW, Idriss IM (2004) Evaluating the potential for liquefaction or cyclic failure of silts and clays. Report No. UCD/CGM-04/01, University of California at Davis, California, USA
- Boulanger RW, Idriss IM (2012) Probabilistic standard penetration test-based liquefaction-triggering procedure. *J Geotech Geoenviron Eng ASCE* 138(10):1185–1195. doi:[10.1061/\(ASCE\)GT.1943-5606.0000700](https://doi.org/10.1061/(ASCE)GT.1943-5606.0000700)
- Boulanger RW, Idriss IM (2014) CPT and SPT based liquefaction triggering procedures. Report No. UCD/CGM-14/01, University of California at Davis, California, USA
- Boulanger RW, Idriss IM (2015a) CPT-based liquefaction triggering procedure. *J Geotech Geoenviron Eng ASCE*. doi:[10.1061/\(ASCE\)GT.1943-5606.0001388](https://doi.org/10.1061/(ASCE)GT.1943-5606.0001388)
- Boulanger RW, Idriss IM (2015b) Magnitude scaling factors in liquefaction triggering procedures. *Soil Dyn Earthq Eng* 79:296–303. doi:[10.1016/j.soildyn.2015.01.004](https://doi.org/10.1016/j.soildyn.2015.01.004)
- Boulanger RW, Seed RB (1995) Liquefaction of sand under bidirectional monotonic and cyclic loading. *J Geotech Eng ASCE* 121(12):870–878. doi:[10.1061/\(ASCE\)0733-9410\(1995\)121:12\(870\)](https://doi.org/10.1061/(ASCE)0733-9410(1995)121:12(870))
- Boulanger RW, Ziotopoulou K (2015) PM4Sand (Version 3): a sand plasticity model for earthquake engineering applications vol 1. Report No. UCD/CGM-15, University of California at Davis, California, USA
- Brandes HG, Seidman J (2008) Dynamic and static behavior of calcareous sands. In: The eighteenth international offshore and polar engineering conference, 2008
- Carraro JAH, Bandini P, Salgado R (2003) Liquefaction resistance of clean and nonplastic silty sands based on cone penetration resistance. *J Geotech Geoenviron Eng ASCE* 129(11):965–976. doi:[10.1061/\(ASCE\)1090-0241\(2003\)129:11\(965\)](https://doi.org/10.1061/(ASCE)1090-0241(2003)129:11(965))
- Castro G (1975) Liquefaction and cyclic mobility of saturated sands. *J Geotech Eng Div ASCE* 101(GT6):551–569
- Cetin KO, Bilge HT (2012) Performance-based assessment of magnitude (duration) scaling factors. *J Geotech Geoenviron Eng ASCE* 138(3):324–334. doi:[10.1061/\(ASCE\)GT.1943-5606.0000596](https://doi.org/10.1061/(ASCE)GT.1943-5606.0000596)
- Cetin KO, Seed RB, Der Kiureghian A, Tokimatsu K, Harder LF Jr, Kayen RE, Moss RES (2004) Standard penetration test-based probabilistic and deterministic assessment of seismic soil liquefaction potential. *J Geotech Geoenviron Eng ASCE* 130(12):1314–1340
- Da Fonseca AV, Soares M, Fourie AB (2015) Cyclic DSS tests for the evaluation of stress densification effects in liquefaction assessment. *Soil Dyn Earthq Eng* 75:98–111. doi:[10.1016/j.soildyn.2015.03.016](https://doi.org/10.1016/j.soildyn.2015.03.016)
- De Alba P, Chan CK, Seed HB (1976) Sand liquefaction in large-scale simple shear tests. *J Geotech Eng Div ASCE* 102(GT9):909–927
- Dobry R, Ladd RS, Yokel FY, Chung RM, Powell D (1982) Prediction of pore water pressure buildup and liquefaction of sands during earthquakes by the cyclic strain method, vol 138. NBS Building Science Series 138, US Department of Commerce, Washington, DC, USA
- Finn WD, Pickering DJ, Bransby PL (1971) Sand liquefaction in triaxial and simple shear tests. *J Soil Mech Found Div ASCE* 97(SM4):639–659
- Green RA, Terri GA (2005) Number of equivalent cycles concept for liquefaction evaluations—revisited. *J Geotech Geoenviron Eng ASCE* 131(4):477–488. doi:[10.1061/\(ASCE\)1090-0241\(2005\)131:4\(477\)](https://doi.org/10.1061/(ASCE)1090-0241(2005)131:4(477))
- Idriss IM (1999) An update to the Seed-Idriss simplified procedure for evaluating liquefaction potential. In: Proceeding, TRB workshop on new approaches to liquefaction, Publ. no. FHWA-RD-99-165. Federal Highway Administration, Washington, DC, USA
- Idriss IM, Boulanger RW (2006) Semi-empirical procedures for evaluating liquefaction potential during earthquakes. *Soil Dyn Earthq Eng* 26(2–4):115–130. doi:[10.1016/j.soildyn.2004.11.023](https://doi.org/10.1016/j.soildyn.2004.11.023)
- Idriss IM, Boulanger RW (2008) Soil liquefaction during earthquakes, Monograph. Earthquake Engineering Research Institute (EERI), Oakland
- Idriss IM, Boulanger RW (2010) SPT-based liquefaction triggering procedures. Report No. UCD/CGM-10/02, University of California at Davis, California, USA

- Idriss IM, Boulanger RW (2012) Examination of SPT-based liquefaction triggering correlations. *Earthq Spectra* 28(3):989–1018. doi:[10.1193/1.4000071](https://doi.org/10.1193/1.4000071)
- Ishihara K (1993) Liquefaction and flow failure during earthquakes. *Geotechnique* 43(3):351–451
- Ishihara K (1996) *Soil behaviour in earthquake geotechnics*. Oxford University Press, Clarendon Press, Oxford
- Ishihara K, Yamazaki F (1980) Cyclic simple shear tests on saturated sand in multi-directional loading. *Soils Found* 20(1):45–59
- Ivšić T (2006) A model for presentation of seismic pore water pressures. *Soil Dyn Earthq Eng* 26(2):191–199
- Jiaer WU, Kammerer AM, Riemer MF, Seed RB, Pestana JM (2004) Laboratory study of liquefaction triggering criteria. In: 13th world conference on earthquake engineering, Vancouver, BC, Canada
- Kayen RE et al (2013) Shear-wave velocity-based probabilistic and deterministic assessment of seismic soil liquefaction potential. *J Geotech Geoenviron Eng ASCE* 139(3):407–419
- Kishida T, Tsai C-C (2014) Seismic demand of the liquefaction potential with equivalent number of cycles for probabilistic seismic hazard analysis. *J Geotech Geoenviron Eng ASCE* 140(3):04013023. doi:[10.1061/\(ASCE\)GT.1943-5606.0001033](https://doi.org/10.1061/(ASCE)GT.1943-5606.0001033)
- Kramer SL (1996) *Geotechnical earthquake engineering*. Prentice Hall, Upper Saddle River
- Ladd RS (1974) Specimen preparation and liquefaction of sands. *J Geotech Eng Div ASCE* 100(GT10):1180–1184
- Lee KL, Seed HB (1967) Cyclic stress condition causing liquefaction of sand. *J Soil Mech Found Div ASCE* 93(SM1):47–70
- Liu AH, Stewart JP, Abrahamson NA, Moriwaki Y (2001) Equivalent number of uniform stress cycles for soil liquefaction analysis. *J Geotech Geoenviron Eng ASCE* 127(12):1017–1026. doi:[10.1061/\(ASCE\)1090-0241\(2001\)127:12\(1017\)](https://doi.org/10.1061/(ASCE)1090-0241(2001)127:12(1017))
- Moss RES, Seed RB, Kayen RE, Stewart JP, Der Kiureghian A, Cetin KO (2006) CPT-based probabilistic and deterministic assessment of in situ seismic soil liquefaction potential. *J Geotech Geoenviron Eng ASCE* 132(8):1032–1051. doi:[10.1061/\(ASCE\)1090-0241\(2006\)132:8\(1032\)](https://doi.org/10.1061/(ASCE)1090-0241(2006)132:8(1032))
- Mulilis JP, Seed HB, Chan CK, Mitchell JK, Arulanandan K (1977) Effects of sample preparation on sand liquefaction. *J Geotech Eng Div ASCE* 103(GT2):91–108
- Park T, Park D, Ahn J-K (2014) Pore pressure model based on accumulated stress. *Bull Earthq Eng* 13(7):1913–1926. doi:[10.1007/s10518-014-9702-1](https://doi.org/10.1007/s10518-014-9702-1)
- Peacock WH, Seed HB (1968) Sand liquefaction under cyclic loading simple shear conditions. *J Soil Mech Found Div ASCE* 94(SM3):689–708
- Polito CP (1999) The effects of non-plastic and plastic fines on the liquefaction of sandy soils. Ph.D. Thesis, Virginia Polytechnic Institute and State University
- Seed HB, Peacock WH (1971) Test procedures for measuring soil liquefaction characteristics. *J Soil Mech Found Div ASCE* 97(SM8):1099–1119
- Seed HB, Idriss IM, Makdisi F, Banerjee N (1975) Representation of irregular stress time histories by equivalent uniform stress series in liquefaction analyses. Report No. EERC75-29, Earthquake Engineering Research Center, University of California at Berkeley, USA
- Seed HB, Tokimatsu K, Harder LF, Chung RM (1984) The influence of SPT procedures in evaluating soil liquefaction resistance, vol 15. Report No. UCB/EERC-84, Earthquake Engineering Research Center, University of California at Berkeley, USA
- Seed HB, Tokimatsu K, Harder LF, Chung RM (1985) Influence of SPT procedures in soil liquefaction resistance evaluations. *J Geotech Eng ASCE* 111(12):1425–1445
- Seed R, Moss RES, Krammer AM, Wu J, Pestana JM, Reimer MF, Cetin KO (2001) Recent advances in soil liquefaction engineering and seismic site response evaluation. In: Proceedings on 4th international conference recent advance in geotechnical earthquake engineering. Soil Dynamics, Paper SPL-2.
- Silver ML, Park TK (1976) Liquefaction potential evaluated from cyclic strain-controlled properties tests on sands. *Soils Found* 16(3):51–65
- Silver ML et al (1976) Cyclic triaxial strength of standard test sand. *J Geotech Eng Div ASCE* 102(GT5):511–523
- Sivathayalan S (1994) Static, cyclic and post liquefaction simple shear response of sands. Master thesis, University of British Columbia
- Skandakumar S (2004) Cyclic loading response of Fraser River sand for validation of numerical models simulating centrifuge tests. Master thesis, University of British Columbia
- Tadesse S (2000) Behaviour of saturated sand under different triaxial loading and liquefaction. Ph.D. thesis, Norwegian University of Science and Technology
- Tatsuoka F, Silver ML (1981) Undrained stress-strain behavior of sand under irregular loading. *Soils Found* 21(1):51–66

- Tokimatsu K, Tsutomu Y, Yoshiaki Y (1986) Soil liquefaction evaluations by elastic shear moduli. *Soils Found* 26(1):25–35
- Towhata I (2008) *Geotechnical earthquake engineering*. Springer series in geomechanics and geoengineering. Springer, Berlin. doi:[10.1007/978-3-540-35783-4](https://doi.org/10.1007/978-3-540-35783-4)
- Vucetic M (1994) Cyclic threshold shear strains in soils. *J Geotech Eng ASCE* 120(12):2208–2228. doi:[10.1061/\(ASCE\)0733-9410\(1994\)120:12\(2208\)](https://doi.org/10.1061/(ASCE)0733-9410(1994)120:12(2208))
- Yang J, Sze H (2011) Cyclic behaviour and resistance of saturated sand under non-symmetrical loading conditions. *Géotechnique* 61(1):59–73
- Yoshimi Y, Tokimatsu K, Kaneko O, Makihara Y (1984) Undrained cyclic shear strength of a dense Niigata sand. *Soils Found* 24(4):131–145
- Yoshimi Y, Tokimatsu K, Hosaka Y (1989) Evaluation of liquefaction resistance of clean sands based on high-quality undisturbed samples. *Soils Found* 29(1):93–104
- Zhou YG, Chen YM, Shamoto Y (2009) Verification of the soil-type specific correlation between liquefaction resistance and shear-wave velocity of sand by dynamic centrifuge test. *J Geotech Geoenviron Eng ASCE* 136(1):165–177